

Dynamics of Rotator Chain with Dissipative Boundary

Pu Ke¹ and Zhigang Zheng^{1,*}

¹*Department of Physics and the Beijing – Hong Kong – Singapore Joint Center for Nonlinear and Complex Systems (Beijing), Beijing Normal University, Beijing 100875, People's Republic of China*

We study the deterministic dynamics of rotator chain with purely mechanical driving on the boundary by stability analysis and numerical simulation. Globally synchronous rotation, clustered synchronous rotation, and split synchronous rotation states are identified. In particular, we find that the single-peaked variance distribution of angular momenta is the consequence of the deterministic dynamics. As a result, the operational definition of temperature used in the previous studies on rotator chain should be revisited.

I. INTRODUCTION

The violation of Fourier's law in low dimensional lattice has drawn much attention in recent years due to its fundamental importance to non-equilibrium thermodynamics and statistical mechanics[1]. This phenomenological law, which relies on the local equilibrium hypothesis, is a macroscopic description of non-equilibrium process, and has been verified to be accurate through various experimental settings. However, a rigorous derivation of Fourier's Law from microscopic statistical-mechanical argument is still missing, which motivated a large number of studies on energy conduction in various models. As an unexpected result drawn from these studies, Fourier's Law is violated for the divergence of heat conductivity with system size in many one-dimensional oscillator-based systems, unless the substrate potential exists[2–4] or the interaction potential is asymmetrical[5].

The model of rotator chain was introduced as a counter example to the oscillator-based models. Even without any substrate potential, a 1D rotator chain model, whose interaction potential is also symmetric exhibits normal heat conduction[6, 7]. Nevertheless, when both thermal and mechanical driving exist in this model, the variance profile of momenta, which is commonly used as the operational definition for temperature in the system that involves translational motion[8], is single-peaked[8], this finding seems to directly contradicts Fourier's Law since a necessary condition for a 1D system to comply the law is to have a linear temperature distribution. The origin of this single-peaked distribution was thought to be the interaction between the mechanical forcing and the thermal forcing[8]. Nevertheless, little about the variance of momenta is known when mechanical driving exists exclusively. Although rotator chain model is a special case of the classical XY model, which drawn much attention in the fields of both extensive[9] and non-extensive[10] statistical mechanics, few studies have been focused on the deterministic dynamics of rotator chain, especially the variance profile of angular momenta. Given the interaction potential of rotator chain differs from the oscillator-based models by its periodicity and boundedness, investi-

gation on deterministic dynamics of rotator chain is necessary to further develop the understanding of the energy conduction properties of rotator chain.

The present paper focuses on the deterministic dynamics of the rotator chain with purely mechanical driving. We proved the existence of the globally synchronous rotation and identified two other dynamical states as the parameters vary. The momenta variance profile was observed to be qualitatively similar to the case when both thermal and mechanical driving are presented. As further investigation, we also analyzed the momenta distribution, detailed evolution information, and phase portrait of the interface rotators. The results provided strong evidences that the nonlinear variance profile of angular momenta was of deterministic origin.

The paper is organized as follows. In Sec. II, a detailed description of rotator chain is presented and the existence of the globally synchronous state is proved. Sec. III A discusses energy current, averaged momenta and momenta variance profiles. Sec. III B is devoted to an explanation to the nonlinearity of variance profiles by investigating rotation states of interface rotators. Finally, Sec. IV concludes the paper.

II. ROTATOR CHAIN

A. Description of the Model

A chain of N rotators is described by the angles $\phi = (\phi_1, \phi_2, \dots, \phi_N)$ and their conjugate angular momenta $\mathbf{L} = (L_1, L_2, \dots, L_N)$, See Fig 1. The nearest-neighbor interaction potential is periodical and takes the form

$$U(\phi_k, \phi_{k+1}) = \epsilon [1 - \cos(\phi_{k+1} - \phi_k)], \quad (1)$$

where ϵ is the coupling coefficient.

Moreover, the system is homogeneous, that is, the moments of inertia of all rotator are I . Therefore, the Hamiltonian of the system is

$$\mathcal{H}(\phi, \mathbf{L}) = \sum_k \left\{ \frac{L_k^2}{2I} + \epsilon [1 - \cos(\phi_{k+1} - \phi_k)] \right\}. \quad (2)$$

Dissipation is introduced on the both end for consistency to the case when thermal driving exists (fluctuation-

* zgzheng@bnu.edu.cn

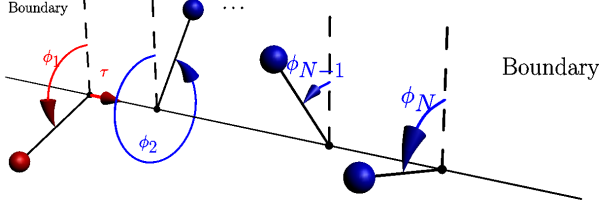


FIG. 1. (Color online) Illustration of a rotator chain.

dissipation theorem). Introducing dimensionless time $s = \sqrt{\epsilon/I}t$ and letting $\omega_k = \frac{d\phi_k}{ds}$, the dimensionless equations of motion with open boundary reads

$$\begin{aligned} \frac{d\phi_k}{ds} &= \omega_k, \\ \frac{d\omega_k}{ds} &= \sin(\phi_{k+1} - \phi_k) - \sin(\phi_k - \phi_{k-1}), \quad k \neq 1, N \\ \frac{d\omega_1}{ds} &= \sin(\phi_2 - \phi_1) - \alpha\omega_1 + \tau, \\ \frac{d\omega_N}{ds} &= -\sin(\phi_N - \phi_{N-1}) - \alpha\omega_N, \end{aligned} \quad (3)$$

where $\alpha = \gamma\sqrt{I/\epsilon}$ is the effective dissipation coefficient and $\tau = T/\epsilon$ is the effective torque, in which γ is the dissipation coefficient and T is the mechanical torque.

B. Dynamical States of Rotator Chain

Based on our analyses and observations, depending on α and τ , the rotator chain has three kinds of dynamical states: *globally synchronous rotation state*, *split synchronous rotation state* and *clustered synchronous state*.

In the globally synchronous rotation states, all rotators rotate at the same angular momentum. It can be proved that (see Sec. II B 2) for any α and $\tau < 2$, i.e. the driving torque is weak while the coupling is strong, the globally synchronous rotation state is unique, and the phase difference between every adjacent rotator pair is $\pi - \arcsin(-\tau/2)$ (cf. (17)).

In the split synchronous rotation state, the driving rotator rotates as if the remaining rotators do not exist, while the remaining rotators rotate slowly in synchronization. This state could be attained when driving torque is sufficiently large.

In the clustered synchronous rotation state, the entire chain is divided into three region: fast rotation region, slow rotation region and interface region. In the fast and slow rotation region, the phase difference between the adjacent rotators oscillates around 0 and could not exceed 2π , while the rotators in the interface region exhibit

complicated dynamical pattern — their rotations are affected by the rotators both in fast rotation region and slow rotation region.

As a preliminary investigation, it is instructive to consider the stability of the system analytically. In the next subsection, the uniqueness of stable fixed point of a rotator chain without dissipation is proved and a saddle-node bifurcation is identified; then the argument is extended to a rotator chain with dissipative boundary to reveal the necessary condition $\tau > 2$ (driving torque is large while coupling is weak) for the forming of nonlinear momenta variance profile.

1. Rotator Chain without Dissipative Boundary

Having introduced phase difference $\delta_k = \phi_{k+1} - \phi_k$ and its derivative $\Delta_k = \frac{d\delta_k}{ds}$, the equations of motion can be cast into ($\alpha = 0$)

$$\begin{aligned} \frac{d\delta_k}{ds} &= \Delta_k, \\ \frac{d\Delta_k}{ds} &= -2\sin\delta_k + \sin\delta_{k-1} + \sin\delta_{k+1}, \quad k \neq 1, N-1 \\ \frac{d\Delta_1}{ds} &= -2\sin\delta_1 + \sin\delta_2 - \tau, \\ \frac{d\Delta_{N-1}}{ds} &= -2\sin\delta_{N-1} + \sin\delta_{N-2}. \end{aligned} \quad (4)$$

The general formula of $\frac{d\Delta_k}{ds} = 0$ is $\sin\delta_k = k\sin\delta_1$, then the only possible solution is $\sin\delta_k = 0$ (i.e. $\delta_k = n_k\pi$). The Jacobian matrix of (4) is

$$\mathbf{J} = \begin{pmatrix} \mathbf{0} & \mathbf{I}_{N-1} \\ \mathbf{C} & \mathbf{0} \end{pmatrix}, \quad (5)$$

where \mathbf{I}_{N-1} is a $N-1$ th order unit matrix, and \mathbf{C} is

$$\begin{pmatrix} -2\chi_1 & \chi_2 & 0 & 0 & \cdots & 0 \\ \chi_1 & -2\chi_2 & \chi_3 & 0 & \cdots & 0 \\ 0 & \chi_2 & -2\chi_3 & \chi_4 & \cdots & 0 \\ \vdots & \vdots & \vdots & \ddots & \ddots & \vdots \\ 0 & 0 & 0 & 0 & \chi_{N-2} & -2\chi_{N-1} \end{pmatrix}, \quad (6)$$

where $\chi_k = \pm 1$. The eigenequation of Jacobian Matrix is

$$\begin{aligned} \det \begin{pmatrix} -\lambda\mathbf{I}_{N-1} & \mathbf{I}_{N-1} \\ \mathbf{C} & -\lambda\mathbf{I}_{N-1} \end{pmatrix} \\ = \det(-\lambda\mathbf{I}_{N-1}) \times \det(-\lambda\mathbf{I}_{N-1} + \mathbf{C}\frac{1}{\lambda}) \\ = (-1)^{N-1} \det(\mathbf{C} - \lambda^2\mathbf{I}_{N-1}) = 0. \end{aligned} \quad (7)$$

Which implies the eigenvalues of \mathbf{J} are square roots of the eigenvalues of \mathbf{C} .

If all $\chi_k = 1$ ($\delta_k = 2n_k\pi$), then the eigenvalues of \mathbf{C} are $\lambda^2 = -2(1 + \cos \frac{k\pi}{N}) < 0$ ($k = 1, \dots, N-1$) [11]. Since λ

are purely imaginary, $\delta_k = 2n_k\pi$ corresponds to a center in phase space.

Suppose that at least one $\chi_r = -1$ ($r < N - 1, \delta_r = (2n + 1)\pi$), then from Gershgorin's Theorem[12], for eigenvalue λ_r^2 of \mathbf{C} , $|\lambda_r^2 - 2| \leq 2$. Because matrix \mathbf{C} is nonsingular (all columns are linear independent), then $\text{Re}\lambda_r > 0$, which renders the fixed point unstable. The argument still holds when more than one $\chi = -1$, since the sum of all off-diagonal elements on arbitrary row is smaller than 2.

As proved above, the only stable fixed point of equation (4) is $\delta_k = 2n_k\pi$, which is a center. The corresponding motion is the collective rotation with the phase difference and its derivative of each pair of rotator oscillate around $(2n_k\pi, 0)$ (libration).

If driving torque is added at the boundary, the general formula of $\frac{d\Delta_k}{ds} = 0$ becomes $\sin \delta_k = k \sin \delta_1 + (k - 1)\tau$. Substituting it into $\frac{d\Delta_{N-1}}{ds} = 0$ gives the necessary condition for the existence of fixed points $\sin \delta_1 = (1 - N)/N\tau$. At the thermodynamic limit, $\lim_{N \rightarrow \infty} \sin \delta_1 = -\tau$, and $\tau = 1$ is a saddle-node bifurcation point.

2. Rotator Chain with Dissipative Boundary

The role of the boundary rotators is of crucial importance in the formation of nonlinear variance profile. Consider a system consists of only two boundary rotators

$$\begin{aligned} \frac{d\delta}{ds} &= \Delta, \\ \frac{d\Delta}{ds} &= -2 \sin \delta - \alpha \Delta - \tau. \end{aligned} \quad (8)$$

Introducing new time scale $\xi = \sqrt{2}s$, then the equation transform to

$$\frac{d^2\delta}{d\xi^2} = -\sin \delta - \eta \frac{d\delta}{d\xi} - \beta, \quad (9)$$

where $\eta = \frac{\sqrt{2}}{2}\alpha$ and $\beta = \frac{\tau}{2}$. Despite the minus sign, equation (9) is the governing equation for the Josephson junction, and received extensive study[13]. Depending on the effective dissipation coefficient η and the effective torque β , we can observe three kinds of bifurcation: homoclinic, infinite-period and saddle-node bifurcations. The saddle-node and the homoclinic bifurcations matter here, if $\beta > 1$ then there is no fixed point in the phase plane, all trajectories are attracted to a unique, stable limit cycle (cf. Fig. 2(c))[14]; limit cycle and stable spiral point could also coexist (bistable state cf. 2(b)) if $\beta < 1$ and η is sufficiently small, but there is no general analytical formula for the homoclinic bifurcation curve. A limit cycle corresponds to the unsynchronized rotation; while when $\beta < 1$, it is possible that two rotator phase-locked (cf. Fig. 2(a)).

The existence of a saddle-node bifurcation point in the rotator chain with boundary rotators will be proved in

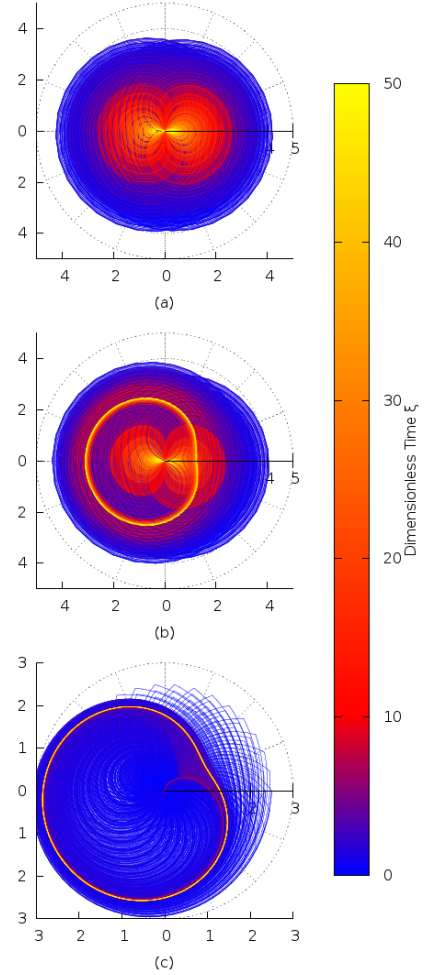


FIG. 2. (Color online) Phase portrait of (9) in polar coordinate, the angle represents phase difference and the radius represents the time derivative of the phase difference. (a) $\eta = 0.1, \beta = 0.027$, only fixed points exist (b) $\eta = 0.1, \beta = 0.037$, bistable state: fixed points and limit cycle coexist (c) $\eta = 0.1, \beta = 1.1$, only limit cycle exist.

the next paragraph and further corroborated by numerical simulation in Sec. III A.

The phase difference equation of (3) is

$$\begin{aligned} \frac{d\delta_k}{ds} &= \Delta_k, \\ \frac{d\Delta_k}{ds} &= -2 \sin \delta_k + \sin \delta_{k-1} + \sin \delta_{k+1}, \quad k \neq 1, N-1 \\ \frac{d\Delta_1}{ds} &= -2 \sin \delta_1 + \sin \delta_2 + \alpha \omega_1 - \tau, \\ \frac{d\Delta_{N-1}}{ds} &= -2 \sin \delta_{N-1} + \sin \delta_{N-2} - \alpha \omega_N, \end{aligned} \quad (10)$$

and the phase difference equation for two boundary ro-

tators ($\delta_{1,N} = \phi_N - \phi_1$) is

$$\begin{aligned}\frac{d\delta_{1,N}}{ds} &= \Delta_{1,N}, \\ \frac{d\Delta_{1,N}}{ds} &= \frac{d\omega_N}{ds} - \frac{d\omega_1}{ds}, \\ &= -\sin\delta_{N-1} + \sin\delta_1 - \alpha\Delta_{1,N} - \tau.\end{aligned}\quad (11)$$

The condition $\frac{d\Delta_k}{ds} = 0$ can be rewritten in the form of a forward and a backward recurrent equation

$$\begin{aligned}\sin\delta_k &= 2\sin\delta_{k-1} - \sin\delta_{k-2} & k \geq 3 \\ \sin\delta_{N-k} &= 2\sin\delta_{N-k+1} - \sin\delta_{N-k+2} & k \geq 3\end{aligned}\quad (12)$$

Solving $\frac{d\Delta_{1,N}}{ds} = 0$ for $\sin\delta_1$ and substituting the result into $\frac{d\Delta_{N-2}}{ds} = 0$ gives the initial value for the backward recurrence equation

$$\begin{aligned}\sin\delta_{N-1} &= -\sin\delta_1 - \tau, \\ \sin\delta_{N-2} &= -2\sin\delta_1 + \alpha\omega_N - 2\tau.\end{aligned}\quad (13)$$

The initial value of the forward recurrence equation is straightforward from $\frac{d\Delta_1}{ds} = 0$

$$\begin{aligned}\sin\delta_1 &= \sin\delta_1, \\ \sin\delta_2 &= 2\sin\delta_1 - \alpha\omega_1 + \tau.\end{aligned}\quad (14)$$

Then the general formulae for forward and backward recurrence equation can be obtained

$$\begin{aligned}\sin\delta_k &= k\sin\delta_1 + (k-1)(\tau - \alpha\omega_1), \\ \sin\delta_{N-k} &= -k\sin\delta_1 - k\tau + \alpha(k-1)\omega_N,\end{aligned}\quad (15)$$

and the necessary condition for fixed points then follows ($\Delta_{1,N} = \omega_N - \omega_1 = 0$)

$$\sin\delta_k + \sin\delta_{N-k} = -\tau. \quad (16)$$

The only solution that satisfies (16) and $\frac{d\delta_k}{ds} = 0$ simultaneously is

$$\sin\delta_k = -\frac{\tau}{2}. \quad (17)$$

According to (17), it is evident that $\tau = 2$ is a saddle-node bifurcation point, if $\tau > 2$, then there could not be any fixed point, and the entire system could not be synchronized. Numerical simulation confirmed that $\tau > 2$ is a necessary condition for nonlinear variance profile to form.

The argument of last subsection still holds, the only differences are $\chi = \pm\sqrt{1 - \frac{\tau^2}{4}}$ and the elements in Jacobian regarding $\Delta_{1,N}$ that render the stable fixed point a spiral.

The above result shows under the condition $\tau < 2$ the rotator chain with dissipative boundary could have the possibility of synchronized collective rotation.

When $\tau > 2$, it can be proved that there exist trajectories of (10) that are confined in the energy shell

E_r . E_r is determined by $\frac{dE}{ds} = \omega_1(\tau - \omega_1) - \omega_N^2 < 0$, if $\omega_1 > \tau$, then the inequality holds under any condition, then $E_r = N(\tau^2/2 + 2)$. The determination of the types of trajectories calls for further studies on Poincaré-Bendixson type theorem in N-dimensional space.

With globally synchronous rotation, nonlinear profile of angular momenta is impossible, since the momentum variance of each rotator is identically 0, which indicate $\tau > 2$ is a necessary condition for the nonlinear profile to form.

III. NUMERICAL SIMULATION

The system of equations (3) had been integrated numerically by Velocity-Verlet and Gear's Predictor-Corrector algorithm[15] for a chain of 1024 rotators with the time step size $\Delta s = 0.01$, while there is some time-step bias, both methods produced the same qualitative results with respect to the choice of the time step.

The variance of momentum and the local energy flux are common observables to investigate the relationship between the temperature gradient and the energy flux in the low-dimensional system. They are calculated in our study to reveal the deterministic dynamics of rotator chain.

The variance of momentum is computed by the standard definition

$$\begin{aligned}\text{var}\{\omega_k\} &= \langle (\omega_k - \langle \omega_k \rangle)^2 \rangle = \langle \omega_k^2 \rangle - \langle \omega_k \rangle^2 \\ &= \lim_{s \rightarrow \infty} \frac{1}{s} \int_0^s \omega_k^2(\zeta) d\zeta - \left[\lim_{s \rightarrow \infty} \frac{1}{s} \int_0^s \omega_k(\zeta) d\zeta \right]^2.\end{aligned}\quad (18)$$

The expression of energy flux could be derived by substituting the equation of motion into the derivative of the local energy and comparing the result to the continuity equation for local energy[1, 16]

$$j_k = \lim_{s \rightarrow \infty} \frac{1}{2s} \int_0^s [\omega_k(\zeta) + \omega_{k+1}(\zeta)] F[\phi_{k+1}(\zeta) - \phi_k(\zeta)] d\zeta. \quad (19)$$

We define the norm of a solution vector to explore the periodicity of the solution. The norm of a solution vector $\mathbf{V} = (\phi)$ is defined to be

$$|\mathbf{V}| = \sqrt{\sum_k (\phi_k^2 + \omega_k^2)}. \quad (20)$$

Note that the norm has the property $|\mathbf{V}| = 0$ if and only if $\mathbf{V} = \mathbf{0}$, this reduces the description of a closed phase trajectory from a high dimensional curve to one dimensional. Since if $|\mathbf{V}(s) - \mathbf{V}(0)|$ returns to 0 periodically, the trajectory $\mathbf{V}(s)$ is a closed orbit.

The fixed boundary conditions were also checked numerically, this is equivalent to adding extra torques $-\sin\phi_k$ ($k = 1, N$) on each end. In particular, a rotator chain with both kinds of boundary condition had the

single-peaked variance profile of momenta in the certain parameter region.

All observables were analyzed for the time steps of $10^8 - 10^{10}$, after the system had relaxed to steady state.

A. An Overview of the Dynamical States

The energy flux is plotted for revealing the overall dynamical states of the rotator chain, see FIG. 3.

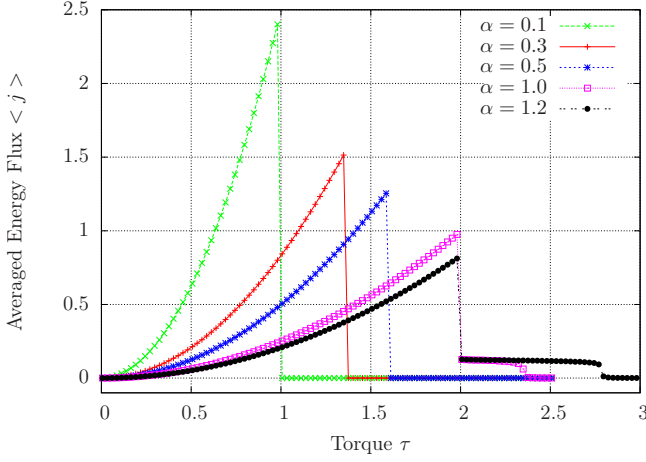


FIG. 3. (Color online) Averaged energy flux of rotator chain.

As the driving torque increased, the torque-flux curve exhibited three qualitatively different segments for all $\alpha > 1$. When $\tau < 2$, the local energy flux increased monotonically with driving torque as $\langle j \rangle = \tau^2/4\alpha$, while identically plunged when $\tau > 2$, and virtually vanished if the mechanical torque is larger than $2.636\alpha - 0.437$ (by linear fit). For the cases $\alpha < 1$, the local energy flux dropped when $\tau < 2$. We have proved rotator chain without dissipative boundary has a saddle-node bifurcation point $\tau = 1$ (cf. IIB1). As the effective dissipation coefficient α decreased, $\frac{d\Delta_1}{ds}$ in transient state could be too large for the globally synchronous rotation (cf. FIG. 2(b)), which rendered the rotator chain in *split synchronous rotation state*.

The monotonic relation between the averaged energy flux and the driving torque is straightforward from the result derived in Sec.IIB2. Assume that the system had relaxed to the spiral, then $\Delta_{1,N} = \omega_N - \omega_1 = 0$ and $\sin \delta_k = \tau/2$. For the total energy E of the system $\frac{dE}{ds} = 0$, the work done by driving torque must be balanced by the dissipation at both end $\tau\omega = 2\alpha\omega^2$, combined with (10) we conclude that at spiral all rotators have same angular momenta $\omega = \tau/2\alpha$. Substituting this result and (17) into (19) leads to the relation $\langle j \rangle = \tau^2/4\alpha$. The proof provides a strong evidence that the monotonically increasing segment represent the globally synchronous rotation state of rotator chain.

The averaged momenta and the variance of momenta are plotted in FIG. 4 to analyze each segment of the

curve for $\alpha = 1.0$ in FIG. 3. As expected, the curves in FIG. 4 that represent the three segments are essentially different. The three kinds of curves in FIG. 4 correspond to *globally synchronous rotation*, *clustered synchronous rotation* and *split synchronous rotation* respectively.

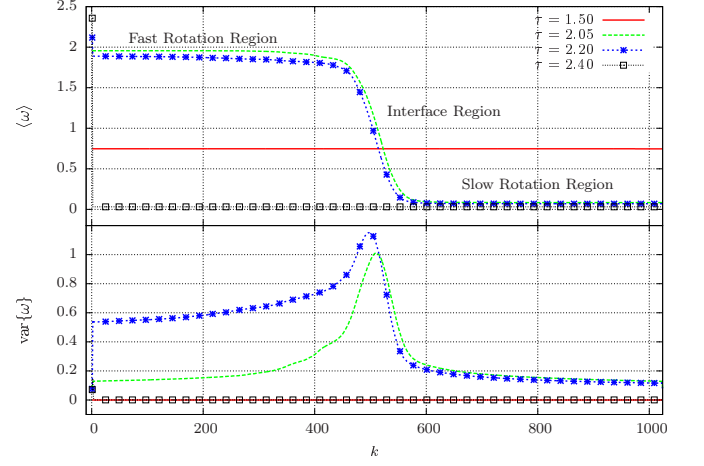


FIG. 4. (Color online) Averaged momenta and variance of momenta for chains of $\alpha = 1.0$.

The entire chain was synchronized when $\tau = 1.5, \alpha = 1.0$, as predicted in IIB2 (Noting that the momentum of every rotator are exactly $\tau/2\alpha$). As the effective torque further increased, an interface area where averaged momenta exhibited significant drop emerged, and the entire chain was divided into three regions: 1. *Fast rotation region* 2. *Interface region* and 3. *Slow rotation region*, the onset of the interface region shifted left slightly as driving torque increased in this state. If the driving torque is sufficiently large, the driving rotator will rotated as if the remaining rotators on the chain do not exist (note that $\omega \approx \tau$), this fact corresponded to the transform from librations to rotations in the single pendulum.

The momenta variance remained 0 when $\tau < 2$ (i.e. the rotator chain was synchronized), which confirm the results derived in IIB. When τ was sufficiently large, only several rotators near the driving rotator had nonzero momenta variance. This fact brought the name *split synchronous rotation state*, despite the first several rotators, the remaining rotators had the same averaged momenta as well as zero variance of momenta, the entire chain thus consists of only one fast moving rotator while the others relaxed to slow synchronous rotation.

The phase trajectory of split synchronous rotation state is a closed orbit while the clustered synchronous rotation state is not. This can be shown by calculating the reduced norm $|\mathbf{V}(s) - \mathbf{V}(s_0)|/\max\{|\mathbf{V}(s) - \mathbf{V}(s_0)|\}$, as shown in FIG. 5. The first two figures represent split synchronous states, and the last one represents clustered synchronous rotation state.

It is interesting to note that the single-peaked distribution of variance existed when the rotator chain was in the *clustered synchronous rotation* state and the peaks lo-

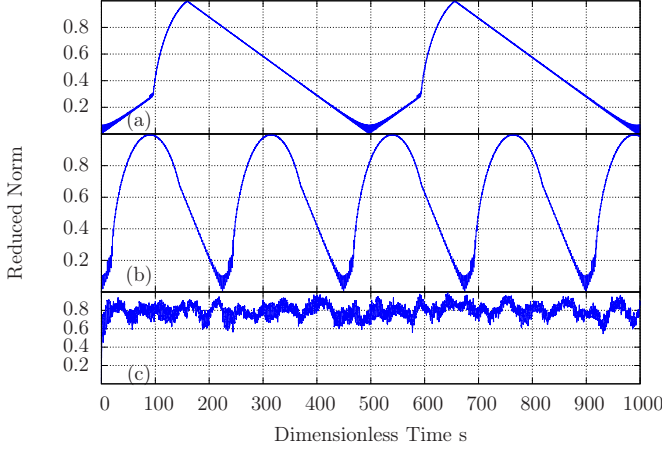


FIG. 5. (Color online) $|\mathbf{V}(s) - \mathbf{V}(s_0)|/\max\{|\mathbf{V}(s) - \mathbf{V}(s_0)|\}$ for (a) $\tau = 1.7, \alpha = 0.5$, (b) $\tau = 2.5, \alpha = 1.0$ and (c) $\tau = 2.2, \alpha = 1.0$.

cated in the interface region. In previous study, this form of variance profile was thought as a consequence of the interaction between the thermal and mechanical driving[8]. However in our model, thermal bath was clearly absent, hence the cause of single-peaked variance profile calls for further investigation by exploring the deterministic dynamical properties of the interface rotators.

B. Rotation States of Interface Rotators

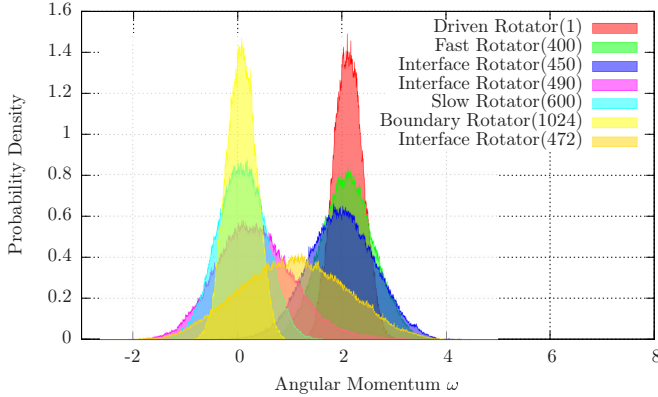


FIG. 6. (Color online) Distribution of angular momenta for $\tau = 2.2, \alpha = 1.0$.

In order to trace the origin of the large variance on the chain it is reasonable to analyze the momentum distribution of the typical rotators. As shown in FIG. 6, the typical rotators in the fast rotation region (e.g 1 and 400) had angular momenta distributions that was symmetrical about the maximum value of angular momentum whereas those in the slow rotation region (e.g 600 and 1024) had

angular momenta distributions around zero. It is interesting to note that the rotators in the interface region (450, 472 and 490) had a momenta distribution extended from the slow rotation region to the fast rotation region, which provided the evidence that the rotators locate in the interface region constantly switched between the slow rotation state and the fast rotation state, which result in large variance.

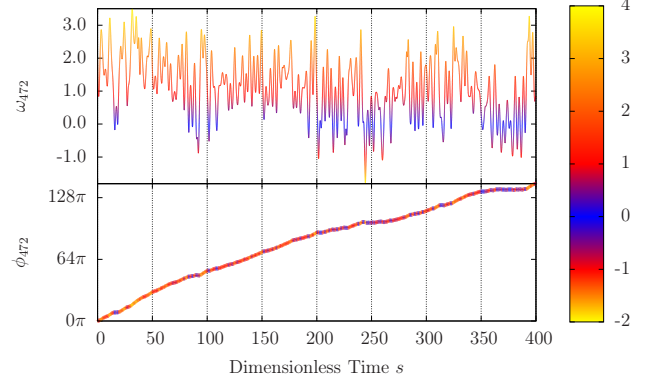


FIG. 7. (Color online) Evolution of angle and angular momentum (rotator 472) for $\alpha = 1.0, \tau = 2.2$.

For a clearer view, the evolution of angular momentum for an interface rotator is plotted in FIG. 7. The oscillation between fast rotation and slow rotation can then be easily spotted.

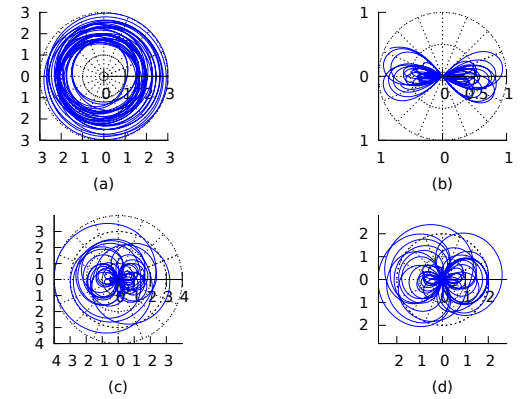


FIG. 8. (Color online) Phase portrait for phase difference between (a) two boundary rotators (b) two adjacent rotators in fast rotation region (c) interface rotator 472 and rotator 471 (d) interface rotator 472 and 473 ($\alpha = 1.0, \tau = 2.2$).

It has been proved in IIB2 that the boundary rotators can not be synchronized when $\tau > 2$, as illustrated in FIG. 8(a). Nevertheless, the adjacent interior rotators had different synchronization states. For the adjacent rotator pairs in either the fast rotation region and the slow

rotation region, the phase difference and its derivative oscillate around $(0, 0)$, which corresponded to the librations in single pendulum (See FIG. 8(b)). The case of rotator pairs in the interface is more complicated, the phase difference between both left and right rotators constantly shifted between librations to rotations and vice versa (See FIG. 8(c) and (d)), which accounted for the oscillations between fast rotation and slow rotation in the interface rotators. Since the rotators in both fast rotation region and the slow rotation region are separately synchronized, and the interface rotators temporarily synchronized to both side, hence the name *clustered synchronous rotation* is designated.

IV. CONCLUSION

The investigations presented above demonstrates that the dynamics of rotator chain with mechanical driving and dissipative boundary depends on the effective driving torque τ and the effective dissipation coefficient α .

Three dynamical states are identified for $\alpha > 1$. *globally synchronous rotation* is proved to exist when $\tau < 2$, i.e. the driving torque is small while the coupling is strong. *split synchronous rotation* state emerges when τ is sufficiently large so that no other rotators on the chain could be synchronize with the driving rotator. *clustered synchronous rotations* result from interior rotators' partial synchronization to each boundary.

The existence of the single-peaked variance profile of momenta is confirmed in the absence of heat bath, and the large variance in the interface region is the consequence of clustered synchronous rotation states, which

emerge when $N > 2$. Temperature is commonly defined as variance of momenta in the research of heat conduction problem in low dimensional system. But as our study shows, the variance profile of momenta could be the consequence of deterministic dynamics exclusively, and has no implication with heat (i.e. stochastic dynamics). Moreover, a rotator chain with mechanical driving has three kinds of dynamical states rather than mere oscillation in the case of oscillator-based systems. Thermal driving could induce transitions between these states, thus whether the operational definition of temperature used in oscillator-based system is appropriate in rotator chain still calls for further investigation.

The deterministic dynamics is essential for understanding the heat conduction properties of the rotator chain when heat baths are added to the system. Heat baths turn the equations of motion of the system from ordinary differential equations to stochastic differential equations. Recent developments on stochastic process reveals that there are correspondences between the deterministic dynamics of a system and its stochastic counterpart when a specific stochastic interpretation other than Itô and Stratonovich is used[17–19]. As a result, it is reasonable to investigate the transport properties of rotator chain by calculating the steady state distribution of the model based on the dynamics of its deterministic counterpart.

ACKNOWLEDGMENTS

This work has been financially supported by grants from the National Natural Science Foundation of China (11075016) and the Foundation for Doctoral Training from MOE.

-
- [1] A. Dhar, *Advances in Physics* **57**, 457 (2008).
 - [2] S. Lepri, R. Livi, and A. Politi, *Phys. Rev. Lett.* **78**, 1896 (1997).
 - [3] G. Casati, J. Ford, F. Vivaldi, and W. M. Visscher, *Phys. Rev. Lett.* **52**, 1861 (1984).
 - [4] A. V. Savin and O. V. Gendelman, *Phys. Rev. E* **67**, 041205 (2003).
 - [5] Y. Zhong, Y. Zhang, J. Wang, and H. Zhao, *Phys. Rev. E* **85**, 060102 (2012).
 - [6] C. Giardinà, R. Livi, A. Politi, and M. Vassalli, *Phys. Rev. Lett.* **84**, 2144 (2000).
 - [7] O. V. Gendelman and A. V. Savin, *Phys. Rev. Lett.* **84**, 2381 (2000).
 - [8] A. Iacobucci, F. Legoll, S. Olla, and G. Stoltz, *Phys. Rev. E* **84**, 061108 (2011).
 - [9] D. R. Nelson and D. S. Fisher, *Phys. Rev. B* **16**, 4945 (1977).
 - [10] C. Anteneodo and C. Tsallis, *Phys. Rev. Lett.* **80**, 5313 (1998).
 - [11] D. Kulkarni, D. Schmidt, and S.-K. Tsui, *Linear Algebra and its Applications* **297**, 63 (1999).
 - [12] R. A. Horn and C. R. Johnson, *Matrix Analysis*, 2nd ed. (Cambridge University Press, 2012).
 - [13] M. Levi, F. Hoppensteadt, and W. Miranker, *Q. Appl. Math.:(United States)* **37** (1978).
 - [14] S. H. Strogatz, *Nonlinear Dynamics And Chaos: With Applications To Physics, Biology, Chemistry, And Engineering (Studies in Nonlinearity)*, 1st ed. (Westview Press, 2001).
 - [15] J. M. Haile, *Molecular Dynamics Simulation: Elementary Methods (Wiley Professional)*, 1st ed. (Wiley-Interscience, 1997).
 - [16] S. Lepri, R. Livi, and A. Politi, *Physics Reports* **377**, 1 (2003).
 - [17] R. Yuan and P. Ao, *Journal of Statistical Mechanics: Theory and Experiment* **2012**, P07010 (2012).
 - [18] R. Yuan, X. Wang, Y. Ma, B. Yuan, and P. Ao, *Phys. Rev. E* **87**, 062109 (2013).
 - [19] Y. Ma, Q. Tan, R. Yuan, B. Yuan, and P. Ao, arXiv preprint arXiv:1208.1654 (2012).